Environmental Research 150 (2016) 73–81

Contents lists available at ScienceDirect

Environmental Research

journal homepage: www.elsevier.com/locate/envres

Interactions of cationic polystyrene nanoparticles with marine bivalve hemocytes in a physiological environment: Role of soluble hemolymph proteins

Laura Canesi [a,*], Caterina Ciacci [b], Rita Fabbri [a], Teresa Balbi [a], Annalisa Salis [c], Gianluca Damonte [c], Katia Cortese [d], Valentina Caratto [a], Marco P. Monopoli [e,f], Kenneth Dawson [e], Elisa Bergami [g], Ilaria Corsi [g]

[a] Dept. of Earth, Environmental and Life Sciences – DISTAV, University of Genoa, Italy
[b] Dept. of Biomolecular Sciences – DIBS, University of Urbino, Italy
[c] Centre of Excellence for Biomedical Research – CEBR, University of Genoa, Italy
[d] Department of Experimental Medicine – DIMES, University of Genoa, Italy
[e] Centre for BioNanoInteractions, School of Chemistry and Chemical Biology, University College Dublin, Ireland
[f] Department of Pharmaceutical and Medical Chemistry, Royal College of Surgeons, 123 St. Stephen Green, Dublin, Ireland
[g] Dept. of Physical, Earth and Environmental Sciences, University of Siena, Italy

ARTICLE INFO

Article history:
Received 7 April 2016
Received in revised form
17 May 2016
Accepted 25 May 2016
Available online 31 May 2016

Keywords:
Nanoplastics
Marine invertebrates
Immunity
Hemocytes
Hemolymph serum
Protein corona

ABSTRACT

The bivalve *Mytilus galloprovincialis* has proven as a suitable model invertebrate for evaluating the potential impact of nanoparticles (NPs) in the marine environment. In particular, in mussels, the immune system represents a sensitive target for different types of NPs. In environmental conditions, both NP intrinsic properties and those of the receiving medium will affect particle behavior and consequent bioavailability/uptake/toxicity. However, the evaluation of the biological effects of NPs requires additional understanding of how, once within the organism, NPs interact at the molecular level with cells in a physiological environment. In mammalian systems, different NPs associate with serum soluble components, organized into a "protein corona", which affects particle interactions with target cells. However, no information is available so far on the interactions of NPs with biological fluids of aquatic organisms.

In this work, the influence of hemolymph serum (HS) on the *in vitro* effects of amino modified polystyrene NPs (PS-NH_2) on *Mytilus* hemocytes was investigated. Hemocytes were incubated with PS-NH_2 suspensions in HS (1, 5 and 50 μg/mL) and the results were compared with those obtained in ASW medium. Cell functional parameters (lysosomal membrane stability, oxyradical production, phagocytosis) were evaluated, and morphological changes were investigated by TEM. The activation state of the signalling components involved in *Mytilus* immune response (p38 MAPK and PKC) was determined. The results show that in the presence of HS, PS-NH_2 increased cellular damage and ROS production with respect to ASW medium. The effects were apparently mediated by disregulation of p38 MAPK signalling. The formation of a PS-NH_2-protein corona in HS was investigated by centrifugation, and 1D- gel electrophoresis and nano-HPLC-ESI-MS/MS. The results identified the Putative C1q domain containing protein (MgC1q6) as the only component of the PS-NH_2 hard protein corona in *Mytilus* hemolymph. These data represent the first evidence for the formation of a NP bio-corona in aquatic organisms and underline the importance of the recognizable biological identity of NPs in physiological exposure medium when testing their potential impact environmental model organisms. Although the results obtained *in vitro* do not entirely reflect a realistic exposure scenario and the more complex formation of a biocorona that is likely to occur *in vivo*, these data will contribute to a better understanding of the effects of NPs in marine invertebrates.

1. Introduction

The development of nanotechnology will inevitably lead to the release of consistent amounts of nanoparticles (NPs) into aquatic environments, in particular in marine ecosystems, with potential

* Corresponding author.
E-mail address: Laura.Canesi@unige.it (L. Canesi).

http://dx.doi.org/10.1016/j.envres.2016.05.045
0013-9351/

adverse effects for aquatic organisms (Baker et al., 2014; Corsi et al., 2014). Invertebrates are emerging as suitable models for evaluating the impact of NPs in marine organisms (Matranga et al., 2012; Corsi et al., 2014; Canesi et al., 2016). The bivalve mollusc *Mytilus* spp. represents so far the most utilized invertebrate model (Canesi et al., 2012; Rocha et al., 2015; Canesi et al., 2016). The application of a battery of functional tests on *Mytilus* immune cells, the hemocytes, has been proven as a powerful tool for the rapid screening of the immunomodulatory effects of different types of NPs in cell models of marine organisms. They also represent robust alternative methods for testing the toxicity of NPs and a possible basis for designing *ecosafe* NP for marine ecosystem sustainability (reviewed in Canesi et al., 2012; Canesi and Procházková, 2013; Corsi et al., 2014).

The effects of NPs on mussel hemocytes were observed at concentrations ranging from 1 to 50 μg/mL in standard conditions utilizing artificial sea water (ASW) as exposure medium (Canesi et al., 2012; Canesi and Procházková, 2013; Canesi et al., 2016). The immunomodulatory effects of NPs were confirmed *in vivo*, in mussels exposed to different types of NPs, in particular using n-TiO_2 as a model NP type, although at much lower concentrations (μg/L). With regards to the *in vivo* exposure conditions, evidence is accumulating that in the aquatic environment NPs can undergo considerable transformation before reaching the target organism (Delay et al., 2012). Not only NP intrinsic properties (core composition, surface charge, size, shape, functionalization, *etc.*), but also those of the receiving medium (pH, ionic strength, natural organic matter) will affect agglomeration/aggregation/settling and consequent bioavailability, uptake and toxicity, in different environments (reviewed in Baker et al., 2014; Corsi et al., 2014; Canesi et al., 2015; Schaumann et al., 2015; Canesi et al., 2016).

However, the evaluation of the biological effects of NPs requires additional understanding of how, once within the organism, NPs interact at the molecular level with cells in a physiological environment, *i.e.* in biological fluids. In mammalian cells, different types of NPs associate with serum soluble components, organized into a "protein corona", which affects particle interactions with target cells (internalization and effects) (Cedervall et al., 2007; Lundqvist et al., 2008; Nel et al., 2009; Fubini et al., 2010; Monopoli et al., 2012; Wang et al., 2013; Fleischer et al., 2014; Treuel et al., 2015; Tenzer et al., 2013). The corona proteins control the specific cellular receptors used by protein-NP complex, the cellular internalization pathways, and the immune response (Wan et al., 2015). Cells recognize the biomolecular corona around a NP, but the biological identity of the complex may be considerably different among mammalian species (Monopoli et al., 2012; Wang et al., 2013; Fedeli et al., 2015).

No information is currently available on NP interactions with cells of aquatic organisms in the presence of biological fluids. The formation of a NP protein corona has been demonstrated so far only in a terrestrial invertebrate, the earthworm *Eisenia fetida*, where soluble coelomic proteins (EfCP) secreted *in vitro* by immune cells, the coelomocytes, form a long-lived corona around AgNPs (Hayashi et al., 2013). Recent data obtained in *Mytilus* hemocytes exposed to cationic polystyrene NPs (PS-NH_2) in the presence of hemolymph serum, suggested that also in marine invertebrates components of biological fluids may affect NP interactions with immune cells (Canesi et al., 2015a). Mussels have an open circulatory system, where the blood (hemolymph) is in direct contact with cells and tissues; therefore, no distinction exists between plasma serum and extracellular medium. The protein composition of *Mytilus* hemolymph serum has been recently characterized (Oliveri et al., 2014; Campos et al., 2015). In this work, the influence of hemolymph serum (HS) on the *in vitro* effects of PS-NH_2 on *Mytilus* hemocytes and the possible formation of NP-protein complexes in HS were investigated.

2. Materials and methods

2.1. Particle characterization

Primary 50 nm amino polystyrene NPs (PS-NH_2), purchased from Bangs Laboratories at 50 μg/mL were previously characterized (Della Torre et al., 2014; Canesi et al., 2015a) in MilliQ water and artificial sea water (ASW). Transmission Electron Microscope-TEM analysis confirmed primary particle nominal size of 50 nm. Dynamic Light Scattering-DLS analysis indicated no agglomeration, and a ζ-potential of $+43 \pm 1$ mV in MilliQ water suspensions. In contrast, in ASW small aggregates were observed (Z-average=200.3 nm, PDI=0.302) and a lower ζ-potential ($+14.2$ mV). For experiments carried out in mussel HS, PS-NH_2 suspensions (50 μg/mL) were freshly prepared in filter sterilized HS and vortexed prior to use. Particle size (Z-average and polydispersity index, PDI) was determined at different times (T0, T 1 h, T 2 h) by DLS (Malvern instruments LTD), using a Zetasizer Nano Series software, version 7.11 (Particular Sciences, UK). Measurements were performed in triplicate samples, each containing 10–14 runs of 10 s for determining Z-average. Samples were also observed by TEM.

2.2. Animals, hemolymph collection, preparation of hemocyte monolayers and hemocyte treatment

Mussels (*Mytilus galloprovincialis* Lam.) 4–5 cm long, sampled from an unpolluted area at Cattolica (RN) were obtained from SEA (Gabicce Mare, PU) and kept for 1–3 days in static tanks containing artificial sea water (ASW) (1 L/mussel) at 16 °C. Sea water was changed daily. Hemolymph was extracted from the posterior adductor muscle of 8–20 mussels, filtered and pooled in 50 mL Falcon tubes at 4 °C and hemocyte monolayers were prepared as previously described (Canesi et al., 2008). Hemocytes were incubated at 16 °C with different concentrations of PS-NH_2 in ASW or filter sterilized hemolymph serum (HS), for different periods of time, depending on the endpoint measured. PS-NH_2 were used at concentrations of 1, 5 and 50 μg/mL (corresponding to 1.46×10^{10}, 7.31×10^{10}, and 7.31×10^{11} particles/mL, respectively), as previously described (Canesi et al., 2015a, 2015b) and in analogy with studies carried out with functionalized PS NPs in human cells (Lunov et al., 2011; Wang et al., 2013). Untreated hemocyte samples (control in ASW or HS) were run in parallel.

2.3. Hemocyte functional assays

Lysosomal membrane stability-LMS, extracellular oxyradical production and phagocytosis were evaluated as previously described (Canesi et al., 2015a, 2015b). LMS in control hemocytes and hemocytes pre-incubated with different concentrations of PS-NH_2 for 30 min was evaluated by the Neutral Red (NR) Retention time assay. The endpoint of the assay was defined as the time at which 50% of the cells showed sign of lysosomal leaking (the cytosol becoming red and the cells rounded). Phagocytosis of neutral red-stained zymosan in 0.05 M Tris–HCl buffer (TBS), pH 7.8, containing 2% NaCl was added to each monolayer at a concentration of about 1:30 hemocytes: zymosan in the presence or absence of PS-NH_2, and allowed to incubate for 1 h. Monolayers were then washed three times with TBS, fixed with Baker's formol calcium (4%, v/v, formaldehyde, 2% NaCl, 1% calcium acetate) for 30 min and mounted in Kaiser's medium for microscopical examination with a Vanox optical microscope. Extracellular oxyradical production was measured by cytochrome *c* reduction. Hemolymph was extracted into an equal volume of TBS (0.05 M Tris–HCl buffer, pH 7.6, containing 2% NaCl). Aliquots (500 μl) of hemocyte suspensions were incubated with 500 μl of cytochrome *c* solution (75 μM

ferricytochrome *c* in TBS), with or without PS-NH_2. Cytochrome *c* in TBS was used as a blank. Samples were read at 550 nm at different times (from 0 to 30 min) and the results expressed as changes in OD per mg protein. For each experiment, control hemocyte samples were run in parallel. Triplicate preparations were made for each sample. All incubations were carried out at 16 °C.

2.4. Transmission electron microscopy

Hemocytes were incubated with PS-NH_2 suspensions (5 μg/mL) in ASW or HS in glass chamber slides (Lab-Tek, Nunc, 177380) for 15 min at 16 °C. Untreated controls were run in parallel. Samples were treated as previously described (Ciacci et al., 2012; Balbi et al., 2013). Cells were washed out in 0.1 M cacodylate buffer in ASW and fixed in the same buffer containing 2.5% glutaraldehyde, for 1 h at room temperature. Cells were postfixed in 1% osmium tetroxide for 10 min and 1% uranyl acetate for 1 h, dehydrated through a graded ethanol series and embedded in epoxy resin (Poly-Bed; Polysciences, Inc., Warrington, PA) overnight at 60 °C. Ultrathin sections (50 nm) were observed with a Tecnai G2 Spirit BioTWIN electron microscope (Philips, Eindhoven, The Netherlands) without additional staining. Digital images were taken with Megaview 3 CCD camera and iTEM software and processed with Adobe Photoshop CS2.

2.5. Electrophoresis and Western blotting

Hemocyte monolayers were incubated with PS-NH_2 suspensions (1.5 mL, final concentration 5 μg/mL) in either ASW or HS at 16 °C for different periods of time. Control hemocytes were run in parallel. Levels of phosphorylated p38 Mitogen Activated Protein Kinase (MAPK) and Proteinkinase C (PKC) in hemocyte protein extracts were determined by SDS–PAGE and Western blotting using phosphospecific antibodies (Canesi et al., 2009; Ciacci et al., 2010). Samples (normalized to 30 μg of protein) were resolved by 12% (for p38 MAPK) or by 10% (for PKC) SDS–polyacrylamide gel electrophoresis (Laemli, 1970). Pre-stained molecular mass markers (Bio-Rad) were run on adjacent lanes. The gels were electroblotted and stained with Coomassie blue (Towbin et al., 1979). Blots were probed with human recombinant-specific, anti-phospho-p38 MAPK (Thr180/Tyr182, New England Biolabs Inc) and anti-phospho-PKC(pan) (ser660, New England Biolabs Inc.) (1:1000) as primary antibodies, and horseradish peroxidase peroxidase- conjugated goat anti-rabbit IgG (Sigma) (1:3000) as secondary antibody. Nitrocellulose membranes were stripped and reprobed with rabbit polyclonal anti-actin antibody (Sigma) (1:1000) as loading controls. Immune complexes were visualized using an enhanced chemiluminescence Western blotting analysis system (Amersham–Pharmacia). Western blot films were digitized (Chemidoc-Biorad) and band optical densities quantified using a computerized imaging system (QuantityOne). Relative optical densities (arbitrary units) at each time point were normalized against those of each control group.

2.6. Isolation of PS-NH_2-protein complexes

Hemolymph was drawn from about 60 mussels and filter sterilized HS was obtained as described above. Due to the low protein content of native HS (about 2 mg/mL), sample concentration was performed in order to ensure full particle coverage. Samples were dialysed overnight at 16 °C against MilliQ water with 10 kDa cutoff tubes, subsequently lyophilized and kept at −80 °C. Samples were resuspended in sterilized ASW and protein content, evaluated following Harthree (1972) was adjusted to 10 mg/mL.

PS-NH_2 were incubated with HS at the nominal particle concentration of 25 μg/mg protein for 24 h at 16 °C on a rocking platform. All experiments were carried out at least twice in duplicates. Parallel samples for field emission scanning microscopy-FESEM analyses were also prepared (see below). After incubation, particle–protein complexes were recovered by centrifugal isolation (Monopoli et al., 2013, with some modifications). Samples were centrifuged at 17,000 × *g* for 75 min at 4 °C. The supernatant was stored at −80 °C (SN) and the pellet was re-suspended in ASW, transferred to a new vial, and centrifuged again to pellet the particle-protein complexes. This washing procedure, used for removing unbound and loosely bound proteins from nanoparticles, was repeated three times, to obtain W1,W2 and W3 samples. The pellet, containing the hard corona (HC) proteins, was re-suspended in 0.1 mL ASW and protein content was evaluated, as well as in SN, W1, W2, W3 samples. W3 samples did not contain any detectable amount of proteins. Samples were added with SDS-sample buffer and boiled for 5 min. Proteins (25 μg) were separated by 10% SDS/PAGE (Pezzati et al., 2015).

2.7. Nano -HPLC-ESI-MS/MS

Bands of interests were cut from the gel and destained, reduced, alkylated and digested with trypsin following Shevchenko et al. (1996) as previously described (Pezzati et al., 2015). Trypsinized peptides were analysed by HPLC-MS/MS using an Ultimate 3000 nano-HPLC system (managed by CHROMELEON software, version 6.70 SP2a, LC Packings, Amsterdam, NL) connected to a Hybrid Quadrupole-Orbitrap mass spectrometer (Q Exactive, Thermo Scientific). Data were submitted to the SEQUEST search engine against Uniprot sequence database for Bivalvia (See Supplementary information).

2.8. Field emission scanning electron microscopy

Samples of PS-NH_2 suspensions in ASW (25 μg/mL) were pelleted by centrifugation and resuspended in MilliQ water, in order to eliminate the excess NaCl. In parallel, samples of the pellet obtained by the centrifugation procedure applied to the PS-NH_2 suspension in HS (25 μg/mg protein/mL) to separate the NP corona proteins, containing PS-NH_2-protein corona complexes (HC), were resuspended in 1 mL of MilliQ water. Both samples were vortexed and two drops of each suspension were placed on a lacey carbon holder and left to dry in air without coating. Samples were observed by field emission scanning electron microscopy (FESEM) on a Zeiss SUPRA 40 VP scanning electron microscope operating at 20 kV.

2.9. Statistical analysis

Data are the mean ± SD (triplicates) of at least 4 independent experiments. Statistical analysis was performed using ANOVA followed by Tukey's post hoc test. Data from Western blot analyses were analysed by the Mann-Whitney *U* test with significance at $p < 0.05$.

3. Results

3.1. Characterization of PS-NH_2 suspensions in different media

DLS analyses were performed to follow agglomeration of PS-NH_2 suspensions (50 μg/mL) in mussel hemolymph serum (HS) at 0, 1 and 2 h (Table 1) and compared with those previously obtained in MilliQ and ASW (Della Torre et al., 2014; Canesi et al., 2015a, 2015b). The formation of small agglomerates was detected in HS, with Z-average and PDI values in the range of 178–186 nm

Table 1
DLS analysis of PS-NH_2 suspensions (50 μg/mL) in different media, showing Z-average (nm) and polydispersity index (PDI). HS: *Mytilus* hemolymph serum (0.22 μm filtered). Data on HS are reported at different times of incubation (0, 1 and 2 h). Data are reported as mean ± SD. MQ: Milli-Q water; ASW: artificial sea water.

	Z-average (nm)	PDI
HS T_0	178 ± 2	0.37 ± 0.01
HS T_1	179 ± 1	0.35 ± 0.01
HS T_2	186 ± 3	0.34 ± 0.05
MQ[a]	57 ± 2	0.07 ± 0.02
ASW[a]	200 ± 6	0.30 ± 0.02

[a] Data from Canesi et al. (2015a, 2015b).

and 0.34–0.37, respectively, from 0 to 2 h (Table 1, Fig. S1a). A representative TEM image of PS-NH_2 suspensions in HS is reported in Fig. S1b. The slightly smaller size of these agglomerates with respect to those formed in ASW (200 nm) (Table 1) may be due to the lower pH of HS (7.3) with respect to that of ASW (8.0), as well as to the presence of organic serum components in HS. No agglomeration was observed in MilliQ water.

3.2. Effects of HS on responses of mussel hemocytes to PS-NH_2

The effects of PS-NH_2 suspensions in HS on hemocyte functional parameters were evaluated in comparison with ASW medium and the results are shown in Fig. 1. As previously reported (Canesi et al., 2015a, 2015b), short term incubation (30 min) of hemocytes with PS-NH_2 suspensions in HS induced a large and dose-dependent decrease in LMS (from −30% with respect to controls) at 1 μg/mL); much smaller effects were observed in ASW medium (Fig. 1a). In particular, at 5 μg/mL the decrease in LMS was 15% in ASW and about 50% in HS. In addition, stimulation of extracellular ROS production was two-fold higher in HS than in ASW both at 5 and 50 μg/mL (Fig. 1b). In both exposure media, PS-NH_2 induced a general decrease in phagocytic activity. However, only in HS a significant effect could be observed also at the lowest concentration tested (−20% at 1 μg/mL) (Fig. 1c).

In Fig. 2 representative TEM images of control hemocytes and hemocytes incubated for 15 min with 5 μg/mL PS-NH_2 in ASW or HS are reported. Control hemocytes with several intracellular granules and intact elongated filopodia were observed, both in HS (Fig. 2a) and in ASW (not shown). Exposure to PS-NH_2 induced rapid morphological alterations in hemocytes: in ASW, loss of filopodia as well as appearance of plasma membrane blebs were observed, together with the presence of large vacuoles (Fig. 2b). Similar, but more evident alterations were observed in hemocytes incubated with PS-NH_2 in HS, characterized by the presence of swollen cytoplasmic extensions (blebbed pseudopodia) (Fig. 2c and d). In both conditions, no cellular uptake of individual PS-NH_2 or their agglomerates could be observed.

The effects of PS-NH_2 suspensions in HS and ASW on signalling components involved in hemocyte activation were evaluated, and the results are reported in Fig. 3. Hemocytes were incubated for different periods of time (from 10 to 60 min) with PS-NH_2 (5 μg/mL) and the phosphorylation state of the stress activated p38 MAPK and of PKC was evaluated in cell protein extracts by electrophoresis and Western blotting with specific anti-phospho-MAPK or anti-phospho-PKC(pan) antibodies. Fig. 3a and b show representative blots of p-p38 and p-PKC obtained after incubation with PS-NH_2 in ASW or HS. Densitometry analysis of phosphorylated protein bands showed a progressive decrease in p38 MAPK phosphorylation in ASW (−55% with respect to controls at 60 min). On the other hand, in the presence of HS, PS-NH_2 induced a time dependent increase in p-p38 levels, that was maximal (up to 2,5 folds with respect to controls) at 60 min (Fig. 3c). PKC phosphorylation was evaluated utilizing anti-pan-phospho-PKC antibodies, that recognize two phosphorylated protein bands of ~70 and 75 kDa, respectively, in mussel hemocytes as already reported in mammalian cells (Canesi et al., 2006a, 2006b; Ciacci et al., 2010). In ASW, PS-NH_2 induced a transient increase in phosphorylation of both PKC bands at 30 min (+75% with respect to control). On the contrary, in the presence of HS, significant decreases in the levels of p-PKC were observed at 30 and 60 min (−25% and −20% of controls, respectively) (Fig. 3d).

3.3. Isolation of PS-NH_2 protein complexes and protein identification by nano-HPLC-ESI-MS/MS

PS-NH_2 suspensions in HS were subjected to a basic protocol utilized to isolate the NP-corona proteins in mammalian serum (centrifugation, 1D gel electrophoresis, MS) (Monopoli et al., 2013) with slight modifications. A representative gel is reported in Fig. 4. In lane 2 the classical protein separation profile of whole *Mytilus* serum (WS) is reported, characterized by the absence of proteins of MW higher than 100 kDa and by a major protein band around 35–30 kDa (Oliveri et al., 2014; Pezzati et al., 2015). A similar pattern was observed in the supernatant obtained from the first centrifugation of the PS-NH_2 suspension in HS (SN). The procedure

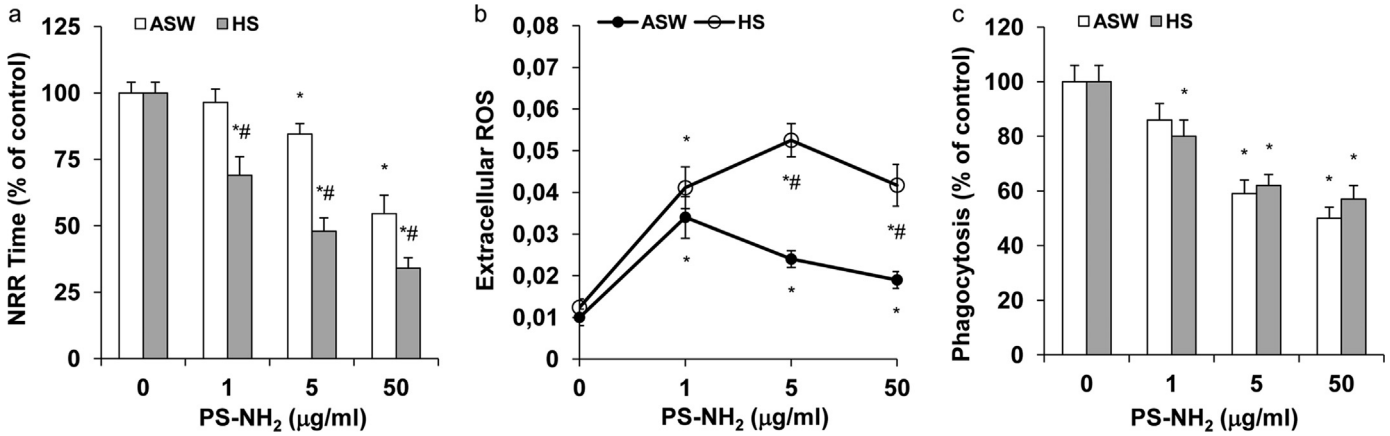

Fig. 1. Effects of PS-NH_2 suspensions in different media on hemocyte functional parameters. Cells were incubated as described in methods with PS-NH_2 suspensions (1, 5, 50 μg/mL) in either ASW or in HS. (a) lysosomal membrane destabilization, evaluated as NR retention time; (b) extracellular oxyradical production, evaluated as cytochrome *c* reduction. (c) phagocytic activity, evaluated as uptake of Neutral-Red conjugated zymosan particles. Data, expressed as percent of control values (untreated hemocytes) and representing the mean ± SD of four experiments in triplicate, were analysed by ANOVA followed by Tukey's post hoc test ($p \leq 0.05$). *=all treatments *vs* controls; #=serum *vs* ASW.

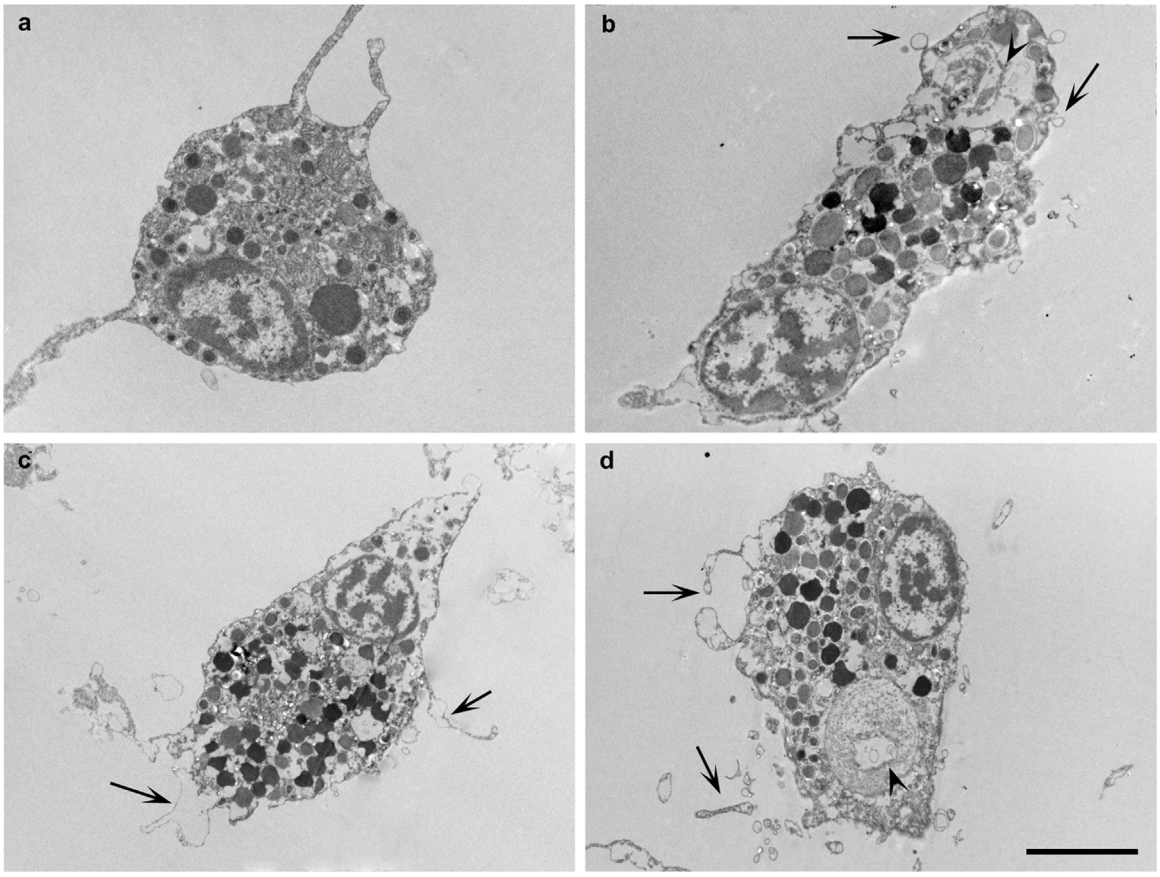

Fig. 2. Electron microscopy of *Mytilus* hemocytes. Representative TEM images of control and PS-NH_2 exposed cells (15 min, 5 μg/mL) in the presence of ASW or HS. Scale bar 5 μm. (a) Control granular hemocyte with intact filopodia, several intracellular granules and well visible mitochondria; (b) hemocyte exposed to PS-NH_2 in ASW, showing loss of filopodia and presence of plasma membrane blebs (arrows), and a large intracellular vacuole (arrowhead). (c, d) Hemocytes exposed to PS-NH_2 in HS, showing short blebbed pseudopodia/enlarged cytoplasmic extensions (arrows), irregular plasma membrane surfaces, a large vacuole (d, arrowhead). Fragments of broken filopodia can be also observed around hemocytes (c).

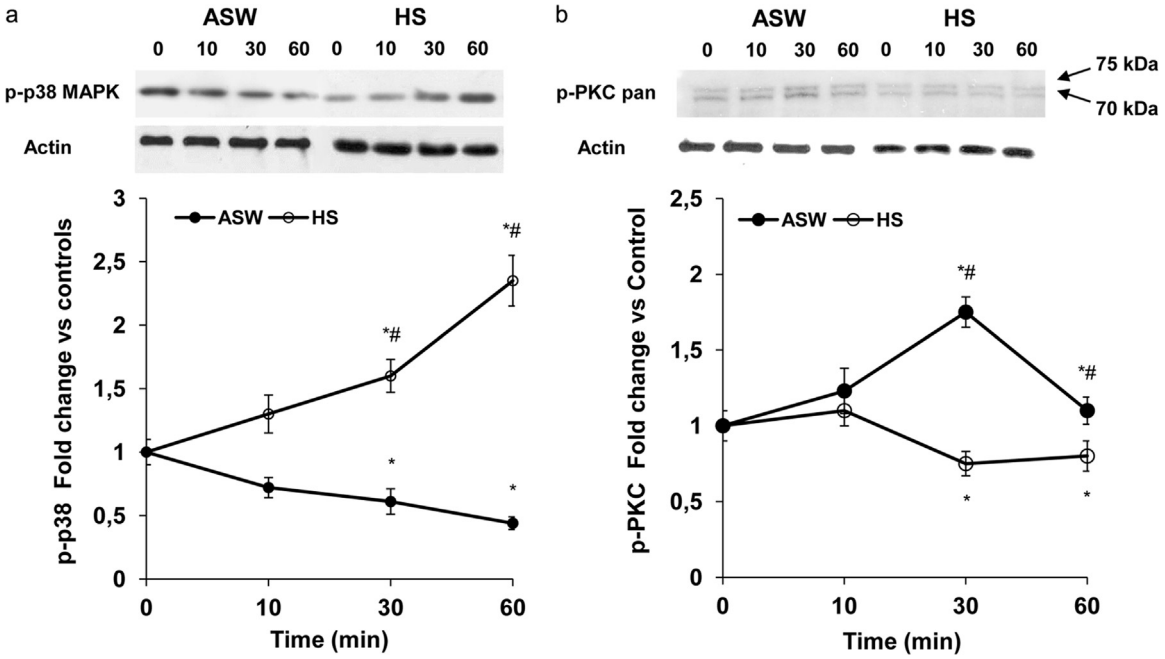

Fig. 3. Effects of incubation of mussel hemocytes with PS-NH_2 (5 μg/mL) for different periods of time (10–60 min) on p38 MAPK and PKC phosphorylation in the presence of ASW or hemolymph serum (HS). C=control. Protein extracts from control and PS-NH_2-treated hemocytes were subjected to 12% SDS-PAGE followed by Western blotting using polyclonal phosphospecific antibodies to p38 MAPK and PKC pan. Bands were detected using enhanced chemiluminescence reagents (see Section 2). Results are representative of three independent experiments. (a, b) representative blot of phosphorylated p38 MAPK and PKC (75 kDa and 70 kDa p-PKC); anti-actin blots are shown as loading controls. (c, d) densitometric analysis of blots from three independent experiments (mean ± SD). Relative increases in band optical densities (arbitrary units) were normalized for the control band in each series. *= $P \leq 0.05$. $p < 0.05$ Mann–Whitney *U* test.

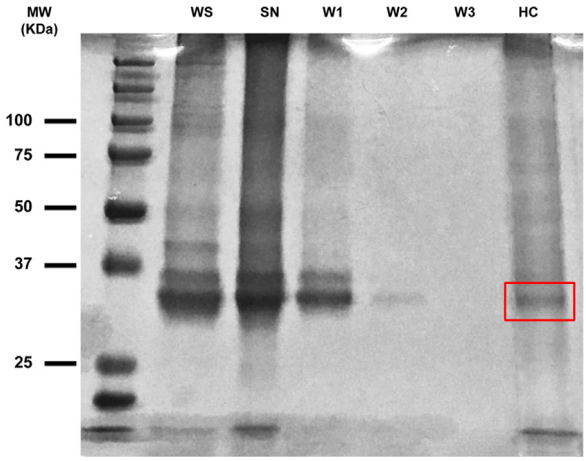

Fig. 4. Separation of PS-NH_2 protein complexes from HS of *M. galloprovincialis* proteins by SDS-PAGE and staining with Coomassie Brilliant Blue. PS-NH_2 were incubated in HS at the nominal concentration of 25 μg NP/mg serum protein/mL, and samples were subjected to repeated centrifugation and washing steps as described in Section 2. A whole serum sample (WS) in the absence of NPs was included (Lane 1). Lane 2: supernatant after the first centrifugation of the PS-NH_2 suspension in HS (SN); Lanes 3–5: samples corresponding to the three washing steps (W1, W2, W3); Lane 6: long-lived, hard corona proteins (HC). A representative gel of three independent experiments is shown. The arrow indicates the position of band excised for tandem mass spectrometry analysis.

resulted in the strong presence of 30–32 kDa protein band in wash 1 (W1) that became attenuated in W2, and was not present in W3, confirming the successful application of the protocol. After the third washing step the supernatant did not contain any detectable amount of proteins. In the final pellet, containing the hard protein corona (HC), a single protein band of the apparent MW of a 32 kDa was observed. Densitometric analysis of this band in all samples indicated that the protein content in the HC sample was about 40% of that present in whole hemolymph serum (Fig. S2).

The 32 kDa band was cut from the gel, trypsin digested and analysed by nano-HPLC-ESI-MS/MS. The results allowed to specifically identify the PN-NH_2 corona protein as the Putative C1q domain containing protein MgC1q6 of *M. galloprovincialis* (F0V443), with high confidence peptides corresponding to a sequence coverage of 75.76% and high sequest score of 423. Details on all the identified peptides (seventeen in total) related with the MgC1q6 protein are reported in Table S1.

3.4. Field emission scanning electron microscopy (FESEM)

FESEM observations were carried out on PS-NH_2 suspensions in ASW (0.25 mg/mL) and in the NP pellet obtained by the centrifugation procedure applied to obtain the PS-NH_2 -protein corona complexes. As shown in a representative image in Fig. 5(a and c), in ASW, agglomerates made up of small clusters or chains of nanosized particles were observed. In samples containing PS-NH_2 -protein corona complexes, individual particles were embedded in an amorphous material forming large agglomerates (about 1 μm in size) (Fig. 5b and d).

4. Discussion

In *Mytilus* hemocytes PS-NH_2 suspensions in ASW medium (1, 5, 50 μg/mL) have been recently shown to induce a dose-dependent decrease in phagocytic activity and increase in lysozyme

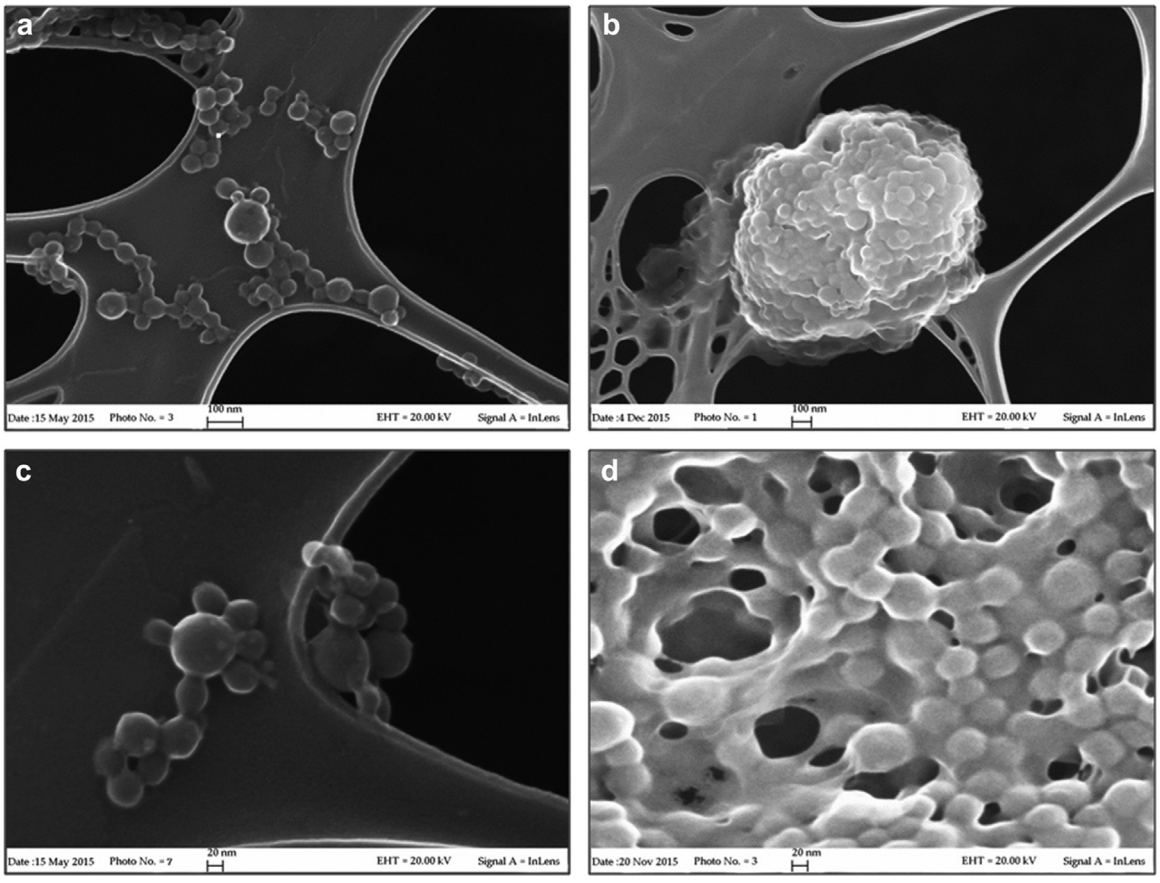

Fig. 5. Representative images obtained by field emission scanning electron microscopy (FESEM) on PS-NH_2 suspensions in ASW (a,c) and in samples of the hard corona proteins (HC) (b,d).

activity; moreover, stimulation of oxyradical and nitric oxide production, was observed, with maximal effects at lower concentrations. Clear signs of cytotoxicity (lysosomal damage and apoptotic processes) were evident only at the highest concentration tested (Canesi et al., 2015a, 2015b). The effects of PS-NH_2 in *Mytilus* hemocytes were comparable with those observed in mammalian cells (Wang et al., 2013), although the responses were particularly rapid, in line with the physiological role of invertebrate immune cells as first line of defence against non-self material (Canesi and Procházková, 2013).

The results of the present work demonstrate that the presence of biological fluids, *i.e.*, hemolymph serum, significantly affects the responses of *Mytilus* hemocytes to PS-NH_2. In order to evaluate particle behavior in exposure medium, DLS analysis of PS-NH_2 suspensions in HS was performed: the results showed the formation of agglomerates of about 180 nm in size that were stable throughout the time frame of hemocyte exposure. This size was slightly smaller than that previously measured in PS-NH_2 suspensions in ASW (Canesi et al., 2015a, 2015b). This slight difference may be due to differences in pH between ASW and HS, as well as to the presence of organic components in HS.

Exposure to PS-NH_2 in HS significantly increased lysosomal membrane destabilization and oxyradical production with respect to ASW exposure medium. TEM analysis indicated that PS-NH_2 in ASW induced rapid cellular damage, in particular at the plasma membrane level (membrane blebbing and loss of filopodia). More extensive damage was observed in HS, with formation of short, blebbed pseudopodia. Large intracellular vacuoles were often seen in both conditions. No uptake of PS-NH_2 agglomerates could be observed in either ASW or HS within the short exposure conditions of the experiment (15 min). These effects were in agreement with the large decrease in phagocytic activity of zymosan particles induced in both conditions at longer times of incubation, indicating an overall disruption of phagocytic/*endo*cytic pathways.

The mechanisms involved in mediating the effects of PS-NH_2 in different exposure media were investigated by evaluating the phosphorylation (activation) state of the stress activated p38 MAPK and of PKC, the main cytosolic kinases involved in the immune function of mussel hemocytes (Canesi et al., 2006a, 2006b; Ciacci et al., 2010). In ASW, PS-NH_2 induced a decrease in p-p38 MAPK levels, and a transient phosphorylation of PKC (both the 75 and 70 kDa isoforms). In contrast, different types of NPs (carbon black and metal oxides) have been previously shown to induce a transient phosphorylation of p38 MAPK (Canesi et al., 2008; Ciacci et al., 2012). In this light, the results show a distinct effect of cationic NPs on p38 MAPK and give a further insight on the specificity of the responses of mussel hemocytes to different types of NPs. Moreover, these data indicate that PKC, in addition to stress-activated MAPK, represents a potential target for NPs.

Distinct effects were observed in the presence of HS, where a persistent increase in phosphorylation of p38-MAPK was observed, whereas the levels of p-PKC were slightly decreased. The extent and time course of activation of p38 MAPK and PKC are crucial in determining the outcome of the response to immune stimuli: in particular, in *Mytilus* hemocytes, transient phosphorylation is associated with efficient activation of the immune response, whereas persistent phosphorylation is generally related to lysosomal damage and immunotoxic effects (Betti et al., 2006; Canesi et al., 2008). The results indicate that the stronger effects of PS-NH_2 on functional parameters and cellular damage observed in the presence of physiological medium are partially mediated by disregulation of p38 MAPK signalling. Overall, these data suggest that the presence of HS components may affect surface interactions between PS-NH_2 and the hemocytes, and consequent activation state of membrane receptors and related signalling pathways, leading to cellular responses distinct from those observed in ASW medium.

In mammalian biological fluids, attachment of proteins and lipids results in the formation of hard and soft coronas around NPs, with long and short typical exchange times, respectively (Rahman et al., 2013; Docter et al., 2015). The lifetime of hard corona has been shown to be of several hours, long enough for many biological and physiological phenomena to occur: therefore, the hard corona defines the biological identity of the particle. The competition between different proteins in mammalian serum for adsorption on the NP surface changes the composition of the corona over time. In most cases, proteins with high abundance in the plasma are first adsorbed on the surface, and over the time, they are replaced by proteins with lower concentration but higher affinity (Rahman et al., 2013). In a first attempt to characterize the possible formation of a hard protein corona in mussel serum, PS-NH_2 were incubated for 24 h in HS, and the suspension was subjected to the standard procedure utilized for mammalian serum (Monopoli et al., 2013), adapted for mussel HS, for separation and identification of NP-protein corona complexes by centrifugation, 1D PAGE and MS. Although further studies are needed to better characterize and identify the corona proteins using more adequate proteomic tools, this procedure allowed for the identification of the only protein associated with PS-NH_2 as the Putative C1q domain containing protein MgC1q6 of *M. galloprovincialis* (F0V443).

A recent proteomics study demonstrated that in *M. galloprovincialis* MgC1q6 (or Extrapallial protein-EP precursor) is the most abundant serum protein, with different bands detected by both 1- and 2-D gel electrophoresis and MS analysis (Oliveri et al., 2014). Shotgun analysis of *Mytilus* hemolymph proteome showed that MgC1q6 has a relative abundance about three times higher in serum than in hemocytes (Campos et al., 2015). MgC1q6 or EP is the same protein previously identified by different methods and named as serum protein band 1-SPB1, histidine-rich glycoprotein-HRG, heavy metal-binding protein-HIP, keystonin (reviewed in Oliveri et al., 2014). It is an acidic glycoprotein with a high histidine content that can bind Ca^{2+} and heavy metals. Recently, by a MS-based approach, a complex and anomalous N-glycan structure was determined in *M. edulis* EP (Zhou et al., 2013). Such unique structure and calcium and heavy metal-binding properties indicate that this protein plays a key role in multiple biological functions including shell formation, metal ion transportation and detoxification (Zhou et al., 2013). Moreover, we have recently demonstrated that MgC1q6 has a key role in immunity, acting as a specific serum opsonin that mediates adhesion and killing of invading bacteria carrying D-mannose-sensitive ligands (Pezzati et al., 2015). These data supported the role of this protein in innate immune response, due to the presence of conserved complement C1q domains (Gerdol et al., 2011).

The results of the present study identify MgC1q6 as the only protein component of the hard corona formed in *M. galloprovincialis* HS around PS-NH_2. Binding of MgC1q6 to PS-NH_2 could be partly due to the positive charges retained by PS-NH_2 in high ionic strength media, as shown by the values of ζ potential recorded in ASW (Canesi et al., 2015a, 2015b). Protein glycosylation may also contribute to interactions with PS-NH_2; glycosylation of the protein corona has been shown to play an important role in maintaining the colloidal stability of NPs in human plasma (Wan et al., 2015).

Overall, the results obtained so far underline the need of understanding how the formation of a NP protein corona may affect the biological outcome of NP exposure, in marine organisms as in mammalian systems. In general, the presence of proteins reduces NP surface energy by nonspecific adsorption, leading to lowered membrane adhesion and uptake efficiency (Lesniak et al., 2013). Therefore, the formation of the protein corona in mammalian serum is considered as a general protective effect from the

potential cytotoxicity of NPs. Similarly, in earthworms, incubation of AgNPs with coelomic proteins lead to formation over time of AgNP-EfCP corona complexes that induced significantly greater NP accumulation in coelomocytes. Therefore, it was hypothesized that NP hard corona proteins function as recognizable molecular patterns, making the NP-protein complexes "visible" for clearance by phagocytic cells (Hayashi et al., 2013). The results obtained in this work indicate that in the marine mussel *Mytilus* the formation of a serum protein corona increases, rather than decrease, the short term *in vitro* toxicity of PS-NH_2 towards immunocytes. Similarly, a recent study reported that a single histidine rich glycoprotein-HRG, present in human (and mouse) plasma, but not in foetal calf serum, forms a stable hard corona around SiO_2-NPs that confers to these particles the ability to evade their capture by macrophages, thus potentially changing their biological fate (Fedeli et al., 2015). In different model organisms, the outcome of the response may depend on the type of NPs, of the target cell, and of the composition of biological fluids, that appears to be species-specific.

Available data on the *in vitro* effects of NPs in marine invertebrate cells were carried out in sea water media, or in common media adjusted for ionic strength and pH (reviewed in Canesi et al., 2016). However, it has been shown that in *Mytilus* hemocytes, responses to cytokines and bacterial challenge were significantly affected by the presence of hemolymph serum, this resulting in activation of distinct signalling components that induce or prevent lysosomal damage and apoptotic processes (Betti et al., 2006; Balbi et al., 2013; Pezzati et al., 2015). The present data demonstrate the additional role of hemolymph serum in the interactions with PS-NH_2.

Overall, the results underline the importance of the physiological exposure medium and the determinant role of the recognizable biological identity during *in vitro* testing of NPs with invertebrate immune cells. However, the protein composition of extracellular fluids of invertebrates is largely unknown, given the large diversity of phyla and species, and different proteins may be involved in the formation of a stable corona around different NPs in different invertebrate groups (marine, freshwater, terrestrial). In earthworm coelomocytes, lysenin was identified as the major corona protein for AgNP *in vitro* (Hayashi et al., 2013), and different secreted proteins related to cell-to-cell signalling were identified in *Daphnia magna* (Nasser and Lynch, 2015). In mussels, MgC1q6 may play a key role in the interactions occurring *in vivo* between the hemolymph and not only PS-NH_2, but also other types of NPs. As in earthworms, different NPs may induce secretion of specific proteins by mussel hemocytes. However, it must be underlined that the results obtained *in vitro* do not entirely reflect a realistic exposure scenario and the more complex formation of a bio-corona that is likely to occur *in vivo* in invertebrate species. Further studies are needed to investigate the formation of NP protein corona in mussels exposed *in vivo* to different types of NPs at concentrations closer to those predicted in the marine environment. Both *in vitro* and *in vivo* studies will contribute to the understanding of NP uptake and potential toxicity in invertebrate species.

Finally, the results obtained with PS-NH_2 provide a further insight on the potential impact of nanoplastics in marine organisms. Occurrence of nanoplastics in the sea and their possible impact on marine biota is obviously part of the growing concern for the continuous increase of plastic wastes and debris in the aquatic compartment, including estuarine and coastal areas (Moore, 2008; Wegner et al., 2012; Mattsson et al., 2015). Polystyrene (PS) is one of the most largely used plastics worldwide, accounting for 24% of the macroplastics in the estuarine habitat, and it can be found in the oceans and in marine biota as micro- and nano-debris (Browne et al., 2008; Moore, 2008; Andrady, 2011; Plastic Europe, 2013). Recent data reported the formation over time (from 14 days) of nanoplastics of about 220 nm by degradation of polystyrene in controlled conditions (Lambert and Wagner, 2016). In the sea urchin embryo (*Paracentrotus lividus*), exposure to PS NPs, in particular PS-NH_2, caused severe developmental defects and induced changes in gene expression suggesting the involvement of apoptotic pathways (Della Torre et al., 2014). A recent study in brine shrimp larvae (*Artemia franciscana*) showed that PS NPs might affect food uptake (feeding), behavior (motility) and physiology (multiple molting) (Bergami et al., 2016). PS-NH_2 cause developmental defects and changes in gene expression also in *Mytilus* embryos (Canesi et al., 2015b, and ms. in preparation). Taken together, the results underline the potential impact of nanoplastics from the molecular to the organism and population level in marine invertebrates. In this light, knowledge of their interactions with cells within the physiological environment of model species represents the basis for understanding their fate and impact on marine biota.

Author contributions

L.C. and I.C. designed the research and supervised the project; C.C., R.F., T.B., E.B. performed the research and analysed the data; L. C. analysed the data and wrote the paper; L.C., I.C., K.D. and M.M. supervised the paper.

Additional information

Competing financial interests: The authors declare no competing financial interests.

Funding sources

This work was partly supported by the Italian Ministry of Research (PRIN2009FHHP2W) Marine ecotoxicology of nanomaterials: toxicity and bioaccumulation of nanotitanium dioxide in edible species in the presence of metals and dioxin.

Acknowledgements

The Authors thank Dr. Laura Negretti and Dr. Michele Montagna (DISTAV) for their invaluable technical assistance in FESEM analyses and preparation of mussel samples.

Appendix A. Supplementary material

Supplementary data associated with this article can be found in the online version at http://dx.doi.org/10.1016/j.envres.2016.05.045.

References

Andrady, A.L., 2011. Microplastics in the marine environment. Mar. Pollut. Bull. 62, 1596–1605.
Baker, T.J., Tyler, C.R., Galloway, T.S., 2014. Impacts of metal and metal oxide nanoparticles on marine organisms. Environ. Pollut. 186, 257–271.
Balbi, T., Fabbri, R., Cortese, K., Smerilli, A., Ciacci, C., Grande, C., Vezzulli, L., Pruzzo, C., Canesi, L., 2013. Interactions between *Mytilus galloprovincialis* hemocytes and the bivalve pathogens *Vibrio aestuarianus* 01/032 and *Vibrio splendidus* LGP32. Fish Shellfish Immunol. 35, 1906–1915.
Bergami, E., Bocci, E., Vannuccini, M.L., Monopoli, M., Salvati, A., Dawson, K.A., Corsi, I., 2016. Nano-sized polystyrene affects feeding, behavior and physiology of brine shrimp *Artemia franciscana* larvae. Ecotoxicol. Environ. Saf. 123, 18–25.

Betti, M., Ciacci, C., Lorusso, L.C., Canonico, B., Falcioni, T., Gallo, G., Canesi, L., 2006. Effects of tumour necrosis factor alpha TNFalpha on *Mytilus* haemocytes: role of stress-activated mitogen-activated protein kinases (MAPKs). Biol. Cell 98, 233–244.

Browne, M.A., Dissanayake, A., Galloway, T.S., Lowe, D.M., Thompson, R.C., 2008. Ingested microscopic plastic translocates to the circulatory system of the mussel, *Mytilus edulis* (L.). Environ. Sci. Technol. 42, 5026–5031.

Campos, A., Apraiz, I., da Fonseca, R.R., Cristobal, S., 2015. Shotgun analysis of the marine mussel Mytilus edulis hemolymph proteome and mapping the innate immunity elements. Vol. 15, pp. 4021–4029.

Canesi, L., Prochàzovà, P., 2013. The invertebrate immune system as a model for investigating the environmental impact of nanoparticles. In: Boraschi, D., Duschl, A. (Eds.), Nanoparticles and the Immune System. Acad. Press, Oxford, pp. 91–112.

Canesi, L., Corsi, I., 2016. Effects of nanomaterials on marine invertebrates. Sci. Total Environ. 2016, 21. http://dx.doi.org/10.1016/j.scitotenv.2016.01.085.

Canesi, L., Betti, M., Ciacci, C., Lorusso, L.C., Pruzzo, C., Gallo, G., 2006a. Cell signalling in the immune response of mussel hemocytes. Invert. Surv. J. 3, 40–49.

Canesi, L., Ciacci, C., Fabbri, R., Marcomini, A., Pojana, G., Gallo, G., 2012. Bivalve molluscs as a unique target group for nanoparticle toxicity. Mar. Environ. Res. 76, 16–21.

Canesi, L., Ciacci, C., Lorusso, L.C., Betti, M., Guarnieri, T., Tavolari, S., Gallo, G., 2006b. Immunomodulation by 17b-estradiol in bivalve hemocytes. Am. J. Physiol. Regul. Integr. Comp. Physiol. 291, R664–R673.

Canesi, L., Ciacci, C., Betti, M., Fabbri, R., Canonico, B., Fantinati, A., Marcomini, A., Pojana, G., 2008. Immunotoxicity of carbon black nanoparticles to blue mussel hemocytes. Environ. Int. 34, 1114–1119.

Canesi, L., Ciacci, C., Bergami, E., Monopoli, M.P., Dawson, K.A., Papa, S., Canonico, B., Corsi, I., 2015a. Evidence for immunomodulation and apoptotic processes induced by cationic polystyrene nanoparticles in the hemocytes of the marine bivalve *Mytilus*. Mar. Environ. Res. 111, 34–40.

Canesi, L., Ciacci, C., Bergami, E., Monopoli, M.P., Dawson, K.A., Canonico, B., Fabbri, R., Corsi, I., 2015b. Effects of cationic polystyrene nanoparticles on the hemocytes and embryo development of *Mytilus galloprovincialis*. In: Proceedings of the 18th International Symposium of Pollutant responses in marine Organisms (PRIMO), Trondheim, Norway, May 2015. ⟨http://www.primo18.com/abstractbook.cfm⟩.

Cedervall, T., Lynch, I., Lindman, S., Berggård, T., Thulin, E., Nilsson, H., Dawson, K.A., Linse, S., 2007. Understanding the nanoparticle-protein corona using methods to quantify exchange rates and affinities of proteins for nanoparticles. Proc. Natl. Acad. Sci. USA 104, 2050–2055.

Ciacci, C., Citterio, B., Betti, M., Canonico, B., Roch, P., Canesi, L., 2009. Functional differential immune responses of *Mytilus galloprovincialis* to bacterial challenge. Comp. Biochem. Physiol. B Biochem. Mol. Biol. 153, 365–371.

Ciacci, C., Betti, M., Canonico, B., Citterio, B., Roch, P., Canesi, L., 2010. Specificity of anti-Vibrio immune response through p38 MAPK and PKC activation in the hemocytes of the mussel *Mytilus galloprovincialis*. J. Invert. Pathol. 105, 49–55.

Ciacci, C., Canonico, B., Bilaničovă, D., Fabbri, R., Cortese, K., Gallo, G., Marcomini, A., Pojana, G., Canesi, L., 2012. Immunomodulation by different types of N-oxides in the hemocytes of the marine bivalve *Mytilus galloprovincialis*. PLoS One 7, e36937.

Corsi, I., Cherr, G.N., Lenihan, H.S., Labille, J., Hassellov, M., Canesi, L., Dondero, F., Frenzilli, G., Hristozov, D., Puntes, V., Della Torre, C., Pinsino, A., Libralato, G., Marcomini, A., Sabbioni, E., Matranga, V., 2014. Common strategies and technologies for the ecosafety assessment and design of nanomaterials entering the marine environment. ACS Nano 8, 9694–9709.

Delay, M., Frimmel, F.H., 2012. Nanoparticles in aquatic systems. Anal. Bioanal. Chem. 402, 583–592.

Della Torre, C., Bergami, E., Salvati, A., Faleri, C., Cirino, P., Dawson, K.A., Corsi, I., 2014. Accumulation and embryotoxicity of polystyrene nanoparticles at early stage of development of sea urchin embryos *Paracentrotus lividus*. Environ. Sci. Technol. 48, 12302–12311.

Docter, D., Strieth, S., Westmeier, D., Hayden, O., Gao, M., Knauer, S.K., Stauber, R.H., 2015. No king without a crown–impact of the nanomaterial-protein corona on nanobiomedicine. Nanomedicine 10, 503–519.

Fedeli, C., Segat, D., Tavano, R., Bubacco, L., De Franceschi, G., de Laureto, P.P., Lubian, E., Selvestrel, F., Mancin, F., Papini, E., 2015. The functional dissection of the plasma corona of SiO_2-NPs spots histidine rich glycoprotein as a major player able to hamper nanoparticle capture by macrophages. Nanoscale 7, 17710–17728.

Fleischer, C.C., Payne, C.K., 2014. Nanoparticle-cell interactions: molecular structure of the protein corona and cellular outcomes. Acc. Chem. Res. 47, 2651–2659.

Fubini, B., Ghiazza, M., Fenoglio, I., 2010. Physico-chemical features of engineered nanoparticles relevant to their toxicity. Nanotoxicology 4, 347–363.

Gerdol, M., Manfrin, C., De Moro, G., Figueras, A., Novoa, B., Venier, P., Pallavicini, A., 2011. The C1q domain containing proteins of the Mediterranean mussel *Mytilus galloprovincialis*: a widespread and diverse family of immune-related molecules. Dev. Comp. Immunol. 35, 635–643.

Harthree, E.F., 1972. Determination of protein. A modification of the Lowry method that gives a linear photometric response. Anal. Biochem 48, 422–427.

Hayashi, Y., Miclaus, T., Scavenius, C., Kwiatkowska, K., Sobota, A., Engelmann, P., Scott-Fordsmand, J.J., Enghild, J.J., Sutherland, D.S., 2013. Species differences take shape at nanoparticles: protein corona made of the native repertoire assists cellular interaction. Environ. Sci. Technol. 47, 14367–14375.

Laemli, U.K., 1970. Cleavage of structural proteins during the assembly of the head of bacteriophage T4. Nature 227, 680–685.

Lambert, S., Wagner, M., 2016. Characterisation of nanoplastics during the degradation of polystyrene. Chemosphere 145, 265–268.

Lesniak, A., Salvati, A., Santos-Martinez, M.J., Radomski, M.W., Dawson, K.A., Åberg, C., 2013. Nanoparticle adhesion to the cell membrane and its effect on nanoparticle uptake efficiency. J. Am. Chem. Soc. 135, 1438–1444.

Lundqvist, M., Stigler, J., Elia, G., Lynch, I., Cedervall, T., Dawson, K.A., 2008. Nanoparticle size and surface properties determine the protein corona with possible implications for biological impacts. Proc. Natl. Acad. Sci. USA 105, 14265–14270.

Lunov, O., Syrovets, T., Loos, C., Nienhaus, U., Mailänder, V., Landfester, K., Rouis, M., Simmet, T., 2011. Amino-functionalized polystyrene nanoparticles activate the NLRP3 inflammasome in human macrophages. ACS Nano 5, 9648–9657.

Matranga, V., Corsi, I., 2012. Toxic effects of engineered nanoparticles in the marine environment: model organisms and molecular approaches. Mar. Environ. Res. 76, 32–40.

Mattsson, K., Hansson, L.A., Cedervall, T., 2015. Nano-plastics in the aquatic environment. Environ.Sci. Process. Impacts 17 (10), 1712–1721.

Monopoli, M.P., Aberg, C., Salvati, A., Dawson, K.A., 2012. Biomolecular coronas provide the biological identity of nanosized materials. Nat. Nanotechnol. 7, 779–786.

Monopoli, M.P., Pitek, A.S., Lynch, I., Dawson, K.A., 2013. Formation and characterization of the nanoparticle-protein corona. Methods Mol. Biol. 1025, 137–155.

Moore, C.J., 2008. Synthetic polymers in the marine environment: a rapidly increasing, long-term threat. Environ. Res. 108, 131–139.

Nasser, F., Lynch, I., 2015. Secreted protein eco-corona mediates uptake and impacts of polystyrene nanoparticles on *Daphnia magna*. J. Proteom. . http://dx.doi.org/10.1016/j.jprot.2015.09.005

Nel, A.E., Mädler, L., Velegol, D., Xia, T., Hoek, E.M., Somasundaran, P., Klaessig, F., Castranova, V., Thompson, M., 2009. Understanding biophysicochemical interactions at the nano-bio interface. Nat. Mater. 8, 543–557.

Oliveri, C., Peric, L., Sforzini, S., Banni, M., Viarengo, A., Cavaletto, M., Marsano, F., 2014. Biochemical and proteomic characterisation of haemolymph serum reveals the origin of the alkali-labile phosphate (ALP) in mussel (*Mytilus galloprovincialis*). Comp. Biochem. Physiol. Part D. Genom. Proteom. 11, 29–36.

Pezzati, E., Canesi, L., Damonte, G., Salis, A., Marsano, F., Grande, C., Vezzulli, L., Pruzzo, C., 2015. Susceptibility of *Vibrio aestuarianus* 01/032 to the antibacterial activity of *Mytilus* haemolymph: identification of a serum opsonin involved in mannose-sensitive interactions. Environ. Microbiol. 17, 4271–4279.

Plastics Europe, 2013. Plastics – The Facts 2013: An Analysis of EuropeAn Latest Plastics Production, Demand and Waste Data. ⟨http://www.plasticseurope.org/Document/plastics-the-facts-2013.aspx⟩.

Rahman, M., Laurent, S., Tawil, N., Yahia, L., Mahmoudi, M., 2013. Nanoparticle and protein corona (Chapter 2). Martinac, B. (Ed.), Protein-Nanoparticle Interactions, the Bio-nano Interface. Springer Series in Biophysics, Springer Berlin Heidelberg, pp. 21–44, ISBN 978-3-642-37555-2.

Rocha, T.L., Gomes, T., Sousa, V.S., Mestre, N.C., Bebianno, M.J., 2015. Ecotoxicological impact of engineered nanomaterials in bivalve molluscs: an overview. Mar. Environ. Res. 111, 74–88.

Schaumann, G.E., Philippe, A., Bundschuh, M., Metreveli, G., Klitzke, S., Rakcheev, D., Grün, A., Kumahor, S.K., Kühn, M., Baumann, T., Lang, F., Manz, W., Schulz, R., Vogel, H.J., 2015. Understanding the fate and biological effects of Ag- and TiO_2-nanoparticles in the environment: The quest for advanced analytics and interdisciplinary concepts. Sci. Total Environ. 535, 3–19.

Shevchenko, A., Jensen, O.N., Podtelejnikov, A.V., Sagliocco, F., Wilm, M., Vorm, O., Mortensen, P., Shevchenko, A., Boucherie, H., Mann, M., 1996. Linking genome and proteome by mass spectrometry: large-scale identification of yeast proteins from two dimensional gels. Proc. Natl. Acad. Sci. USA 93, 14440–14445.

Tenzer, S., Docter, D., Kuharev, J., Musyanovych, A., Fetz, V., Hecht, R., Schlenk, F., Fischer, D., Kiouptsi, K., Reinhardt, C., Landfester, K., Schild, H., Maskos, M., Knauer, S.K., Stauber, R.H., 2013. Rapid formation of plasma protein corona critically affects nanoparticle pathophysiology. Nat. Nanotechnol. 8, 772–781.

Towbin, H., Staehelin, T., Gordon, J., 1979. Electrophoretic transfer of proteins from polyacrylamide gels to nitrocellulose sheets: procedure and some applications. Proc. Natl. Acad. Sci. USA 72, 4350–4354.

Treuel, L., Docter, D., Maskos, M., Stauber, R.H., 2015. Protein corona – from molecular adsorption to physiological complexity. Beilstein J. Nanotechnol. 6, 857–873.

Wan, S., Kelly, P.M., Mahon, E., Stöckmann, H., Rudd, P.M., Caruso, F., Dawson, K.A., Yan, Y., Monopoli, M.P., 2015. The "sweet" side of the protein corona: effects of glycosylation on nanoparticle-cell interactions. ACS Nano 9, 2157–2166.

Wang, F., Yu, L., Monopoli, M.P., Sandin, P., Mahon, E., Salvati, A., Dawson, K.A., 2013. The biomolecular corona is retained during nanoparticle uptake and protects the cells from the damage induced by cationic nanoparticles until degraded in the lysosomes. Nanomedicine 9, 1159–1168.

Wegner, A., Besseling, E., Foekema, E.M., Kamermans, P., Koelmans, A., 2012. Effects of nanopolystyrene on the feeding behavior of the blue mussel (*Mytilus edulis* L.). Environ. Toxicol. Chem. 31, 2490–2497.

Zhou, H., Hanneman, A.J., Chasteen, N.D., Reinhold, V.N., 2013. Anomalous N -glycan structures with an internal fucose branched to GlcA and GlcN residues isolated from a mollusk shell-forming fluid. J. Proteome Res. 12, 4547–4555.